Structure of ^{44}Ti and the Role of Single-Particle Energies and the $T = 0$ Two-Body Interaction in the Development of Rotational Properties in Nuclei*

K. H. Bhatt† and J. B. McGrory
Oak Ridge National Laboratory, Oak Ridge, Tennessee 37830
(Received 4 January 1971)

The structure of low-lying states in ^{44}Ti is studied in terms of a conventional shell model. The calculated spectrum is in reasonable agreement with available experimental information. The results of the "exact" shell-model calculation are compared with calculations of the ^{44}Ti spectrum in terms of the stretch scheme and the deformed Hartree-Fock with projection scheme. We find that these two approximations are not in good agreement with the exact calculation. We study the effects on the calculated spectrum of varying the single-particle energy spectrum. We find that the "rotational" character of the calculated spectrum is sensitive to the single-particle energies. The sensitivity can be accounted for by assuming that the wave functions of the members of a rotational band are projections from an intrinsic state with a strong quadrupole deformation. The effect of the $T = 0$ part of the residual interaction, and of the Pauli principle, on the rotational character of the calculated spectrum of low-lying states is discussed.

I. INTRODUCTION

A subject of long-standing interest in nuclear physics is the relationship between microscopic and collective descriptions of nuclear phenomena. One region of the Periodic Table in which investigations into this question have been made is in the lower end of the s-d shell. ^{20}Ne is one nucleus which has received particular attention. This interest has been stimulated by the fact that many of the observed features of the structure of ^{20}Ne at low excitation energies can be rather well described in terms of collective rotational models, while at the same time the structure of ^{20}Ne is amenable to various microscopic many-particle models. From the observed sequence of spins in ^{20}Ne, the low-lying spectrum has been interpreted in terms of five rotational bands.[1] The structure of ^{20}Ne has been studied in terms of an SU_3 model,[2] and in terms of various deformed Hartree-Fock calculations.[3] Conventional shell-model calculations of ^{20}Ne have been made.[4] In these, an inert ^{16}O core is assumed and the four active particles are distributed in the s-d shell single-particle orbits. These various microscopic models have all been able to display "rotational" behavior. Thus, ^{20}Ne has been a very useful theoretical laboratory in which to study how a many-body system might develop collective properties.

^{44}Ti is the f-p shell analog of ^{20}Ne. In terms of a conventional shell model, it consists of two neutrons and two protons outside an inert ^{40}Ca core. Is the structure of ^{44}Ti similar to the structure of ^{20}Ne; i.e., does it display properties which can be described as rotational? What are the features of the calculations which lead to significant differences in the structure of the two nuclei? In this paper, we discuss the results of a conventional shell-model calculation of ^{44}Ti. An inert ^{40}Ca core is assumed, and the $f_{7/2}$, $p_{3/2}$, $f_{5/2}$, and $p_{1/2}$ orbits are included in the active space. We find that ^{44}Ti does not display obviously rotational features. We compare the shell-model results with the results of a projected Hartree-Fock calculation[5] of ^{44}Ti, and with a shell-model calculation on a truncated basis in which the truncation is made in terms of the so-called stretch scheme of Danos and Gillet.[6] We find that both of these approximation schemes lead to results in poor agreement with the shell-model results. Finally, we discuss a series of shell-model calculations of ^{44}Ti which are aimed at determining what role the single-particle energy spectrum and the $T = 0$ part of the effective two-body interaction play in determining whether or not the shell-model calculation gives results which display rotational properties.

In Sec. II, we discuss the details of the shell-model calculation. In Sec. III we discuss the results of the calculation, and compare them with the existing experimental information on ^{44}Ti. In Sec. IV, we compare the shell-model results with the results of a projected Hartree-Fock calculation and stretch-scheme calculations of ^{44}Ti. In Sec. V, we discuss the effects of varying parts of the effective interaction on the character of the calculated results. In Sec. VI, we summarize the results of this paper.

II. DESCRIPTION OF THE CALCULATION

All the calculations we have made have been in the framework of the conventional shell model.

An inert ^{40}Ca core is assumed, and we include the $0f_{7/2}$, $1p_{3/2}$, $0f_{5/2}$, and $1p_{1/2}$ single-particle orbits in the active space. In this model, ^{44}Ti is described as four particles outside the ^{40}Ca core. We include all Pauli-allowed states of all possible configurations of four particles in the f-p shell orbits in the model vector space. In this space, we diagonalize an effective one-body-plus-two-body Hamiltonian. The resulting eigenvalues we associate with the energy levels in ^{44}Ti. The eigenvectors are associated with wave functions for ^{44}Ti states, and are used to calculate various relevant observables. The construction and diagonalization of the matrices in these calculations were carried out with the use of the Oak Ridge-Rochester shell-model computer programs.[7]

The effective one-body operator is specified by four single-particle energies (s.p.e.). We deduce these s.p.e. from the spectrum[8] of ^{41}Ca. The exact values which we used are

$$\epsilon_{7/2} = -8.36\ ,$$
$$\epsilon_{3/2} = -6.29\ ,$$
$$\epsilon_{5/2} = -2.00\ ,$$
$$\epsilon_{1/2} = -4.00\ .$$

The two-body part of the effective Hamiltonian can be specified by 195 two-body matrix elements. We use the set of matrix elements derived by Kuo and Brown[9] from the Hamada-Johnston nucleon-nucleon interaction for the f-p shell region of the Periodic Table. This set of matrix elements was designed for a space in which the $0g_{9/2}$ orbit is also included in the active model space as well as the four f-p shell orbits. The $g_{9/2}$ orbit probably lies at least as high in energy as the $f_{5/2}$ orbit. Since the parity of this g orbit is opposite to the f-p orbits, any configuration with any active $g_{9/2}$ particles which can contribute to the positive parity levels of ^{44}Ti must have at least two particles in the $g_{9/2}$ orbit. Thus, these configurations would be at rather high energies in zero order. If we included the $g_{9/2}$ orbit in the active space, the matrices would become prohibitively large, and we would also introduce problems associated with spurious center-of-mass motion.[10] The $T=1$ part of the Kuo-Brown interaction was used in a study of the structure of the calcium isotopes.[11] It was shown there that the only significant effect of including two-particle excitations to the $g_{9/2}$ orbit was to slightly depress the ground state relative to the excited spectra. We, therefore, feel that the omission of the $g_{9/2}$ level from the calculations discussed here is not a serious one.

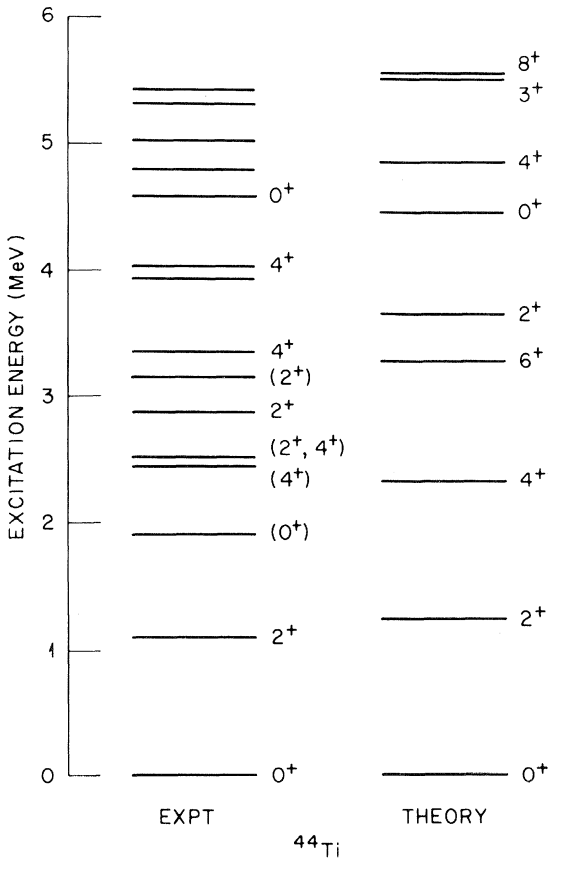

FIG. 1. Calculated and observed spectrum of ^{44}Ti. The calculated results are those obtained with the "realistic" interaction of Kuo and Brown and experimental single-particle energies. The observed spectrum is composited from Ref. 12. All observed and calculated states up to the highest energy state shown are included in the figure.

III. DISCUSSION OF THE CALCULATED SPECTRUM OF ^{44}Ti

The spectrum of ^{44}Ti which is calculated with the model described above is shown in Fig. 1. In the calculated spectra shown, all states calculated to be below the 8^+ state at 5.57 MeV are shown. Also shown in Fig. 1 is the experimental spectrum[12] of ^{44}Ti.

The calculated spectrum does not exhibit a clearly rotational ground-state band. The excitations up to the first 6^+ state are equally spaced as opposed to the $J(J+1)$ spacing of the rigid rotor. The spin assignments in the experimental spectrum are still too uncertain to allow any detailed comparison of theory with experiment. The only definite statement which can be made is that the observed 0^+-2^+ splitting is reproduced by the calculation to within 180 keV. If the observed state at 2.44 is a 4^+ state, then this state is also accounted for by the calculation.

The state observed at 1.90 MeV is the first state

not accounted for by the shell-model calculation. There is one obvious possible explanation for this state. In the observed spectrum[13] of ^{40}Ca, which nucleus we have treated as a closed core, the first excited state is a 0^+ state at 3.35 MeV. This state is some sort of multiparticle multihole or deformed state. In ^{42}Ca, there is an excited 0^+ state observed at 1.84 MeV. This state is not accounted for by the conventional shell-model calculation.[11] A reasonable interpretation is that this state is the result of a coupling of the lowest shell-model 0^+ state in ^{42}Ca to a deformed 0^+ state in the ^{40}Ca core. In ^{44}Ca, there is a 0^+ state at 1.89 MeV in the experimental spectrum. There is evidence[11] that this 0^+ state is probably not a shell-model state, and that it, too, represents a coupling of the shell-model ground state to a deformed state in ^{40}Ca. Thus, it is an obvious extension of this pattern to identify the 1.90-MeV state in ^{44}Ti as the coupling of the shell-model ground state of ^{44}Ti to a deformed 0^+ level in ^{40}Ca.

It is tempting to account for the 2.52-MeV 2^+ level in ^{44}Ti in a similar fashion. In ^{40}Ca, there is an excited 2^+ level at 3.90 MeV, 550 keV above the deformed 0^+ state. In ^{42}Ca there is a $J=2^+$ state at 2.42 MeV. This state is 580 keV above the 0^+ state in ^{42}Ca that we have identified as a "deformed" state. In ^{44}Ca, there is a 2^+ state at 2.66 MeV which could reasonably be called a deformed 2^+ state. This is close enough in energy to the 2.52-MeV level in ^{44}Ti to suggest that the latter also has a strong parentage with an excited state of the ^{40}Ca core. In the absence of any further experimental information, it is difficult to make any other comparisons between the calculated and the observed spectra of ^{44}Ti.

IV. COMPARISON OF SHELL-MODEL, PROJECTED HARTREE-FOCK, AND STRETCH-SCHEME CALCULATIONS OF ^{44}Ti

In this section, we comment on some recent calculations[5] of ^{44}Ti in the so-called stretch scheme, and in terms of projected Hartree-Fock states. Both these calculations were done using, for the residual interaction, a central force with a Yukawa shape and a Rosenfeld exchange mixture, and single-particle energies similar to the ones we have used.

The stretch scheme is a coupling scheme proposed by Danos and Gillet[6] to give a simple microscopic wave function which displays rotational features. The scheme emphasizes neutron-proton correlations in contrast to the usual pairing wave function which emphasizes like-particle correlations. So far the stretch-scheme formalism has been developed only for the cases where there are $2N$ neutrons and $2N$ protons. Given such a situation, N protons and N neutrons are coupled to the maximum total angular momentum allowed by the Pauli principle. The other N neutrons and N protons are similarly coupled, and then the two "chains" are coupled to the total angular momentum of the system.

Khadkikar and Banerjee[5] have calculated the spectrum of ^{44}Ti in a configuration-mixing calculation in which the basis space is truncated by limiting the basis states to stretch-scheme states. The further restriction is made that in any given basis state, both protons are in the same orbit, and both neutrons are in the same orbit. (The stretch-scheme formalism has been developed only for this case, so far.) This restriction has at least one very important consequence, which is that the p-n interaction cannot mix different basis states. (Each basis state differs by at least *two* neutrons or *two* protons.) Those neutron-proton correlations which are not already introduced into the wave function by the choice of representation are thus eliminated from the calculation. Khadkikar and Banerjee also carried out a projected Hartree-Fock (PHF) calculation. They found that the general character of the spectra of low-lying states of ^{44}Ti as calculated in the PHF and stretch models was similar. However, the stretch-scheme spectrum was compressed with respect to the PHF spectrum. The ground-state energy of the PHF solution was -12.5 MeV as compared with -8.2 MeV in the stretch scheme.

We have repeated the complete shell-model calculation of ^{44}Ti in the (f,p) shell with the same interaction as the one used by Khadkikar and Banerjee. The resulting "exact" spectrum is shown in Fig. 2. We also show there the PHF spectrum and the $T=0$ stretch-scheme spectrum. The main similarity between the three calculated spectra is that the spectra of the "ground-state-band" levels all show marked deviations from the $I(I+1)$ spectrum of the rigid rotator. The main qualitative difference in the ground-state bands in the three calculations is that the 8^+ state is much too compressed in both the PHF and stretch-scheme spectrum. The PHF calculation is a significantly poorer approximation to the exact calculation here than in ^{20}Ne.[3] The PHF calculation is essentially a "rotational" calculation. The fact that ^{20}Ne looks much more like a rotational nucleus than ^{44}Ti is certainly a significant factor in the better results of PHF in ^{20}Ne than in ^{44}Ti.

There is a serious breakdown in the agreement between the stretch scheme and the exact calculation for states outside the ground-state band. There is a large gap in the stretch-scheme spectrum, between the ground-state band and the ex-

cited states, which does not exist in the exact calculation. For the excitation spectra, one must conclude that the configuration-mixing in the stretch scheme as performed by Khadkikar and Banerjee is a poor approximation to the exact calculations.

Insofar as the ground-state binding energy is concerned, the exact calculation gives a binding energy of −12.7 MeV. The PHF binding energy of −12.5 MeV is thus in excellent agreement with the exact calculation.

There is little relationship between the wave functions generated in the stretch scheme and in the exact calculation. In Table I, we summarize the composition of the ground-state wave function in the $T=0$ stretch scheme and in the exact calculation. In the stretch scheme, the signature $(f_{7/2}{}^2, p_{3/2}{}^2)$ indicates that there are identical particles in the $f_{7/2}{}^2$ orbit, and identical particles in the $p_{3/2}{}^2$ configuration. The exact calculation was done in the isotopic spin formalism. In that case,

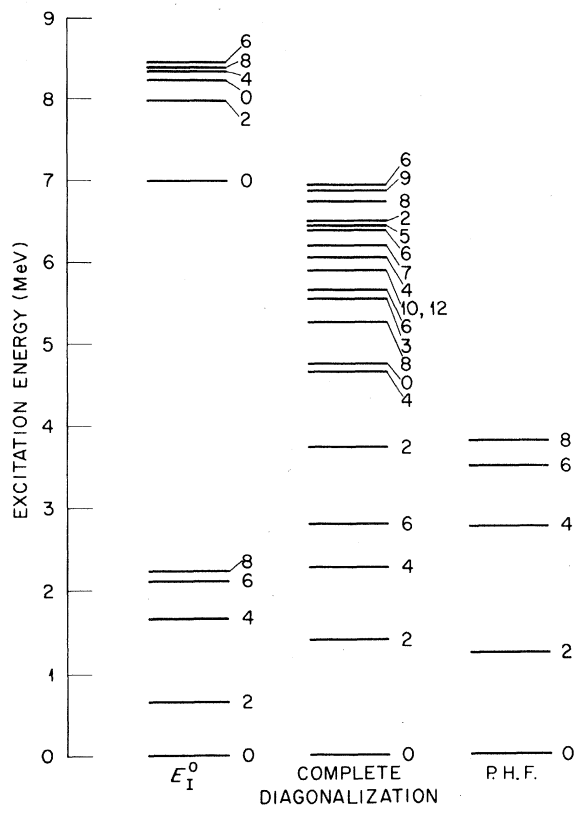

FIG. 2. Calculated spectra of low-lying states of ^{44}Ti in three different models. The first column shows results of stretch-scheme calculations of Khadkikar and Banerjee (Ref. 5), where we show the results for the case where states with good $T=0$ are produced. The second column shows results for complete diagonalization in f-p shell-model space. The third column shows results of a projected Hartree-Fock calculation.

in the configuration $(f_{7/2}{}^2, p_{3/2}{}^2)$ the particles in the $f_{7/2}$ orbit can be like or unlike, as is the case for the $p_{3/2}$ orbit. Thus, the numbers in each column of Table I cannot be compared directly, but as we shall see, this does not prevent us from drawing conclusions as to comparisons of the two wave functions. In the description of the exact wave function, the percentage of j^4 configuration is the sum of all probabilities for all j^4-configuration states in the calculation. In the case of $(j_1{}^2, j_2{}^2)$ configurations, the percentage shown is the sum of all percentages for states of the $[(j_1{}^2,\ T=1), (j_2{}^2,\ T=1)]_J$ which are the only states of the type $(j_1{}^2, j_2{}^2)$ allowed in the stretch scheme. We see that in the stretch scheme, the ground state is almost entirely $f_{7/2}{}^4$ (92%). In the exact ground state, this configuration constitutes less than half of the total wave function. In fact, almost 40% of the exact wave function consists of configurations not even included in the stretch-scheme basis space.

One source of difficulty in the stretch-scheme calculation discussed here is the limitation of like particles to the same orbit. We have already noted that in the representation used here, the p-n interaction cannot connect different basis states. The energy of the state with two protons in the $f_{7/2}$ shell and two neutrons in the $p_{3/2}$ shell lies only 300 keV below the state with a neutron-proton pair in each orbit. In addition, as we pointed out above, 40% of the exact wave function consists of states with an odd number of particles in at least two orbits, and such configurations cannot be included in the stretch-scheme calculation.

Shah and Danos[14] have also reported calculations of ^{44}Ti in the stretch scheme. They use different s.p.e. for neutrons and for protons. Thus, their states do not have good isotopic spin. We are unable to make an exact calculation with their interaction easily since our programs are designed to work with states quantized in isotopic spins.

TABLE I. Composition of 0^+ ground-state wave function of ^{44}Ti in stretch-scheme calculation and complete shell-model calculation. The amplitudes not shown for exact calculation are either not allowed in stretch scheme, or they are less than 0.1 in the ground-state wave function.

Configuration	Stretch scheme (%)	Exact calculation (%)
$f_{7/2}{}^4$	92	46
$(f_{7/2}{}^2,\ T=1)\ (p_{3/2}{}^2,\ T=1)$	1	5
$(f_{7/2}{}^2,\ T=1)\ (f_{5/2}{}^2,\ T=1)$	6	10
$(f_{7/2}{}^2,\ T=1)\ (p_{5/2}{}^2,\ T=1)$	0	1

V. DEVELOPMENT OF ROTATIONAL SPECTRUM

A. Effect of Single-Particle Energies

Since the experimental information on ^{44}Ti is still rather sparse, our primary interest here is in the qualitative nature of the calculated structure of the low-lying states. We have already commented that the calculated spectrum of the low-lying states shows a significant departure from the strict rotational behavior, as opposed to the two-neutron two-proton s-d shell nucleus ^{20}Ne. A tentative explanation of the difference in the behavior of these two spectra is suggested in a letter by Bhatt and Parikh.[15] Their hypothesis can be described briefly as follows. A rotational band of levels will exist if the members of the band can be projected from an intrinsic state with a strong quadrupole deformation. One way to form such a deformed intrinsic state is to construct a determinantal wave function in which the single-particle orbits have large quadrupole moments. The single-particle orbit with the largest possible quadrupole moment in a given space is obtained by diagonalizing the single-particle quadrupole operator in that space. The single-particle orbits of the SU_3 representation are eigenstates of this quadrupole operator. Now assume that the single-major-shell Hartree-Fock procedure gives a good first approximation to the effects of the residual interaction in a given shell model; i.e., assume the two-body interaction generates an effective one-body force in which the active particles move. If this effective Hartree-Fock potential is the quadrupole field; i.e., $V_{\mathrm{HF}} \propto r_i^2 Y^2(\Omega_i)$, then the Hartree-Fock orbits will be identical to the SU_3 orbits. In this case, there will be a strongly deformed intrinsic state, and a rotational spectrum will develop.

The deformation of the self-consistent field is sensitive to *both* the two-body and one-body parts of the residual interaction. The dominant component of the residual interaction is the quadrupole component. If the two-body interaction was pure quadrupole-quadrupole, then a rotational $L(L+1)$ spectrum would result if the spectrum of single-particle states showed an $l(l+1)$ spacing. This can be shown as follows:

Let $Q = \sum_i q_i$ be the total mass quadrupole operator of the nucleons. Then

$$\vec{Q}\cdot\vec{Q} = C - 3\vec{L}\cdot\vec{L}, \tag{1}$$

where C is the SU_3 Casimir operator,[2] and $\vec{L}$ is the angular momentum operator. Then the Hamiltonian

$$H = H_0 - b\vec{Q}\cdot\vec{Q}, \tag{2}$$

where H_0 is the single-particle harmonic-oscillator Hamiltonian and b is a same constant, gives rise to an $L(L+1)$ spectrum. This Hamiltonian can be rewritten as

$$H = H_0 - b\sum_i C_i + 3b\sum_i l_i^2 - 2b\sum_{i<j} q_i\cdot q_j . \tag{3}$$

Here C_i is the SU_3 Casimir operator for a single nucleon. The eigenvalues of C_i are equal for all single-particle states in a major shell. From this expression it is clear that a quadrupole-quadrupole two-body interaction will yield an $L(L+1)$ spectrum if the single-particle spectrum has an $l(l+1)$ spectrum. Empirically, the single-particle potential is such that the single-particle orbit with the largest l value lies lowest in energy. This is due to the large spin-orbit force in the single-particle potential, and to the fact that effects due to the finite size of the well lead to a depression of single-particle orbits with high l. (This effect is introduced in the Nilsson potential by the addition of an attractive l^2 potential.) This situation hinders the two-body interaction from giving rise to rotational spectra.

Let us apply these general arguments to the particular cases of the s-d shell and the f-p shell. If we restrict the calculation to the s-d-shell orbits, the single-particle orbit with the largest mass quadrupole moment has the form $0.82d_0 - 0.58s_0$. (Here d_0 is the single-particle orbit with orbital angular momentum $l=2$ and $l_z=0$.) This orbit contains more d state than s state. If we had performed the Hartree-Fock calculation in a space with the $s_{1/2}$ orbit at 0-MeV excitation, and the $d_{5/2}$ and $d_{3/2}$ orbits at a very high energy, it is hard to conceive of any reasonable residual interaction leading to a lowest Hartree-Fock orbit which contains more d state than s state. In fact, however, in the s-d shell region around ^{16}O the $d_{5/2}$ single-particle orbit lies below and close to the $s_{1/2}$ orbit. This s.p.e. situation favors the generation of Hartree-Fock orbits which are very close to SU_3 orbits. This in turn favors the formation of an intrinsic state for ^{20}Ne with a large quadrupole deformation. Thus, ^{20}Ne displays a rotational spectrum.

Now consider the f-p shell. In a space restricted to f-p-shell orbits, the orbit with the maximum quadrupole moment has the form $0.63f_0$-$0.78p_0$; i.e., this orbit has more p state than f state. The single-particle spectrum which would favor the formation of such an orbit would have the p state below the f state. But, as seen in the observed spectrum[8] of ^{41}Ca, in the lower end of the f-p shell the $f_{7/2}$ orbit is 2 MeV below the $p_{3/2}$ orbit. Thus, one might expect nuclei at the beginning of the f-p shell would not display clearly rotational

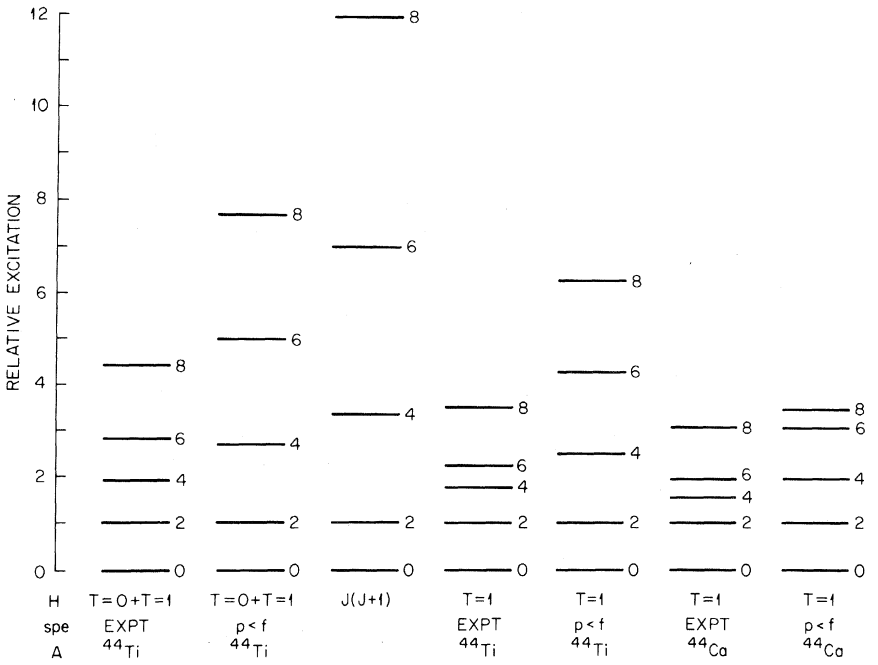

FIG. 3. Calculated spectra of ^{44}Ti and ^{44}Ca in complete f-p shell-model space. In each column a different effective interaction is used, as described in the text. The subheading of each column shows whether (a) just $T=0$ interaction or complete $T=0$ plus $T=1$ interaction is used, (b) what single-particle energy spectra were used, and (c) to what nucleus the spectrum refers. The spectrum labeled $J(J+1)$ is pure rigid rotor predicted spectrum. In all cases the energy scale is renormalized so that the $J=2^+$ state is at 1 MeV.

features. This is consistent with the shell-model results we have found for ^{44}Ti.

As a theoretical experiment, we have repeated the ^{44}Ti calculations with two sets of s.p.e. different from those used in the calculation described above. In one calculation, the $p_{3/2}$ and $p_{1/2}$ orbits were chosen to be degenerate, as were the $f_{7/2}$ and $f_{5/2}$ orbits, with the p doublet 2 MeV below the f doublet. If the argument summarized above is valid, the spectrum calculated with this last s.p.e. spectrum should be more "rotational" than the spectrum calculated with the experimental s.p.e. In Fig. 3, the spectra calculated with the "experimental" s.p.e. and with this altered s.p.e. spectra are shown in the first two columns. In this figure, the spectra have been renormalized so that the first 2^+ state is at 1.0 MeV; i.e., if the calculated 2^+ state is at 2.0 MeV, we divide the excitation energies of all the members of the ground-state "band" by 2. For comparison, we also show in this figure the $J(J+1)$ spectrum of the rigid rotor. We have also calculated, but do not show here, the spectrum which results when *all* single-particle orbits are degenerate. This spectrum is quite similar to the spectrum calculated with the "experimental" s.p.e., although the wave functions in this case are quite different from the wave functions generated with the "experimental" s.p.e. In the calculation in which the p orbits are 2 MeV below the f orbits, a rotational spectrum is clearly present, as predicted in the previous discussion.

We have transformed the j-j coupled wave functions for the ^{44}Ti ground-state band into wave functions expanded in terms of representations of the SU_3 group. For the calculation with the experimental s.p.e., the wave functions display considerable mixing of SU_3 states. For example, the (λ, μ)

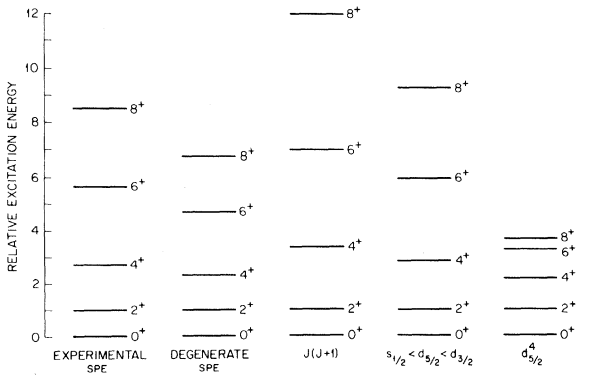

FIG. 4. Calculated spectra of ^{20}Ne in full s-d-shell-model space. See text for details of calculation. The column labeled $J(J+1)$ is pure rigid rotor predicted spectra. In all cases the energy scale is renormalized so that $J=2^+$ state is at 1 MeV.

= (12, 0) state of maximum weight constitutes only 26% of the 0^+ ground state, and there are nine SU_3 states with amplitudes greater than 0.1 in this state. In contrast, in the wave function calculated in the model with the p orbits below the f orbits, the (12, 0) state constitutes 93% of the 0^+ ground state, and there are only two SU_3 states in this wave function with amplitudes greater than 0.1.

The next test we made of the sensitivity of the "rotational" structure to the s.p.e. was for ^{20}Ne. In this case the results are not so dramatic as for ^{44}Ti, and in fact the results are somewhat unexpected. In the ^{20}Ne calculation, we used the following sets of s.p.e.:

	$\epsilon_{5/2}$ (MeV)	$\epsilon_{1/2}$ (MeV)	$\epsilon_{3/2}$ (MeV)
(a)	−4.15	−3.28	+0.93
(b)	0	0	0
(c)	0	−2.0	2.0
(d)	0	∞	∞

Set (a) consists of the experimental s.p.e., the set (b) s.p.e. are degenerate, in set (c) the $s_{1/2}$ is moved below the $d_{5/2}$ and $d_{3/2}$ level, and in set (d) the s.p.e. are such that the states in the ground-state band are pure $d_{5/2}{}^2$ states. The excitation spectra of the ground-state band in ^{20}Ne as calculated with these sets of s.p.e. are shown in Fig. 4. Only the pure $d_{5/2}{}^4$ spectrum does not display any rotational character. The degenerate case is not so different from the experimental case insofar as the $d_{5/2}$-$s_{1/2}$ splitting is concerned, so the rotational result for this case is not so surprising. For the case where the $s_{1/2}$ orbit is below the $d_{5/2}$ orbit by 2 MeV, we see that the ground-state-band spectrum is, if anything, more rotational than is the case when the experimental s.p.e. are used. We pointed out above that in the s-d shell the single-particle orbit with the maximum quadrupole moment contained more d state than s state, so that a spherical single-particle spectrum in which the d orbit is below the s orbit favors the formation of a rotational structure. An inspection of the wave function for the ground state of ^{20}Ne as calculated with the experimental s.p.e. gives a hint as to the cause of this apparent discrepancy. In this wave function the $(d_{5/2}{}^4, J=0)$ state makes up 20% of the total function, and the $(s_{1/2}{}^4, J=0)$ contribution is 3%. Now consider the determinantal wave function for ^{20}Ne formed by putting two neutrons and two protons in the SU_3 orbit with maximum quadrupole moment. Since the SU_3 single-particle orbit contains more d state than s state, this SU_3 intrinsic state contains more d^4 than s^4. It is a straightforward procedure to expand this wave function in j-j coupling as a linear combination of states of good total angular momentum and isotopic spin. The $J=0$ part of this expansion is the 0^+ state projected from the SU_3 intrinsic state. In this projected state the $(s_{1/2}{}^4, J=0)$ state has a larger amplitude than the $(d_{5/2}{}^4, J=0)$ state. This is intuitively reasonable, since the configuration $s_{1/2}{}^4$ is uniquely $J=0$, while the configuration $d_{5/2}{}^4$ is a linear combination of several J values. In the process of projection, the $d_{5/2}{}^4$ strength is spread over several states, while the $s_{1/2}{}^4$ strength all remains in the 0^+ state. Thus, while the intrinsic state has more d^4 than s^4, the process of projection inverts this situation in the 0^+ state. In the shell-model calculation of ^{20}Ne, when we lower the $s_{1/2}$ orbit relative to the $d_{5/2}$ orbit, we enhance the contribution of the $(s_{1/2}{}^4, J=0)$ state to the ground state. This lowering of the $s_{1/2}$ orbit, then, leads to a ground-state 0^+ state which more nearly represents the 0^+ state which is projected from an SU_3 intrinsic state.

The single-particle spectrum can also play a significant role with respect to the so-called "centrifugal stretching" in rotational nuclei. This effect is introduced to account for the observed depression of the energy of the states with high-J values relative to the position predicted by the pure $J(J+1)$ dependence. We have argued that the best theoretical single-particle spectrum for generating rotational spectrum is one in which orbits with small j are lowest in energy. But, experimentally, orbits with high j lie lower than orbits with low j. The states with high total J are dominated by configurations with particles in high-j orbits. In ^{20}Ne, for instance, the 8^+ state is purely $d_{5/2}{}^4$. Such states are very sensitive to the single-particle energies of the high-j orbits, as compared with states with smaller total J which have configurations with particles in all orbits. Thus, the empirically observed lowering of the single-particle orbits with high j contributes to the lowering of high-J states. This effect can be seen in Fig. 4, where we see that the apparent centrifugal stretching effect in ^{20}Ne is reduced when the s orbit is lowered with respect to the d orbit.

B. Enhancement of $E2$ Transitions

We have calculated $B(E2)$ values for transitions between members of the ground-state band in ^{44}Ti and ^{20}Ne. In these calculations we use state-independent one-body effective charges of $0.5e$ for both neutrons and protons (i.e., the total proton charge is $1.5e$ and the total neutron charge is $0.5e$). This prescription has been used previously in the s-d shell,[4] and there is no obvious reason to change it in the f-p shell. The calculated $B(E2)$ values for transitions involving states in the ground-state bands of ^{20}Ne and ^{44}Ti are

summarized in Tables II and III. The *absolute* transition strengths for the $2^+ \rightarrow 0^+$ transitions as calculated with each set of s.p.e. are given. For transitions between higher states in these ground-state bands, the transition strengths *relative* to the strength for the $2 \rightarrow 0$ are given. We also give the relative $B(E2)$ values within a $K=0$ rotational band as calculated in the strong-coupling rotational model.[15] In this case,

$$B(E2)_{J_i \rightarrow J_f} \propto |C^{J_i 2 J_f}_{K\ 0\ K}|^2 .$$

This strong-coupling model is an approximation to the results obtained by an exact projection of states of good angular momentum from a deformed intrinsic state. For ^{20}Ne, there are no striking differences in the $B(E2)$ values calculated with the various different models, with the exception of the absolute value of the $B(E2)$ for the $2 \rightarrow 0$ transition in the pure $d_{5/2}{}^4$ model. This value is roughly $\frac{1}{3}$ of the absolute value for this transition in the other models. Remember that the SU_3 single-particle orbit with the maximum quadrupole moment has the structure $0.82d_0 - 0.58s_0$. Thus, by eliminating the $s_{1/2}$ orbit from the calculation, as is the case in the $d_{5/2}{}^4$ calculation, we significantly reduce the possible maximum value of the quadrupole moment. The significant diminution of the $B(E2)$ value in the $d_{5/2}{}^4$ calculation certainly reflects this fact.

There are more significant differences between the $B(E2)$ values calculated with the different models in ^{44}Ti. We saw the clear development of a rotationlike band in ^{44}Ti when the p orbit was lowered with respect to the f orbit. We see, in the first and second columns of Table II, that the absolute value of the $B(E2)$ for the $2 \rightarrow 0$ transition in the calculation with the lowered p orbits is 40% stronger than in the calculation with the experimental s.p.e. Again this presumably occurs because the lowering of the p orbits leads to low-lying states with larger quadrupole deformations.

TABLE II. Calculated $B(E2)$ values in ^{20}Ne ground-state band for different single-particle energy spectra. Column A shows results with single-particle energies taken from experiment. Column B shows results when single-particle energies are degenerate. Column C shows results when $s_{1/2}$ is moved 2 MeV below $d_{5/2}$. Column D is result for pure $d_{5/2}{}^4$ calculation. The column headed S.C. shows relative values predicted for $B(E2)$ values by the strong-coupling rotational model (Ref. 15).

		$B(E2)\downarrow e^2\text{fm}^4$				
J_i	J_f	A	B	C	D	S.C.
2	0	48	47	52	18	1
4	2	1.24	1.24	1.26	1.13	1.4
6	4	1.01	1.04	1.04	0.93	1.6

We see that in all the models, the relative $B(E2)$ values are reasonably consistent with the strong-coupling values.

C. Effects of the $T=0$ Two-Body Interaction on Collective Behavior

There are reasons for suspecting that the $T=0$ part of the residual two-body force plays an important role in the formation of rotational properties in nuclei. In general, the $T=1$ two-body matrix elements are characterized by large matrix elements between $J=0$ paired states, which states are necessarily spherical. On the other hand, there are usually several strong $T=0$ two-body matrix elements between states with $J \neq 0$. Thus, the $T=0$ interaction is more likely to produce low-lying states which are deformed. Another reason to expect the $T=0$ interaction plays an important role in forming rotational nuclei is suggested again by considering the observed states to be projections from a Slater determinant of deformed single-particle orbits. The most deformed intrinsic state can be found by putting all particles in the orbit with the maximum quadrupole deformation. However, the Pauli principle comes into play, and only one particle of a given species can be

TABLE III. Calculated $B(E2)$ values in ^{44}Ti band. There are three entries in each column heading. H indicates which two-body matrix elements were included in the calculation. s.p.e. characterizes the single-particle spectrum. Expt. indicates s.p.e. taken from experiment were used, $p<f$ indicates p orbits degenerate and 2-MeV below f orbits. The column headed S.C. shows relative strengths as calculated with strong-coupling rotational model (Ref. 15).

					$B(E2)\ e^2\text{fm}^4$				
		H	$T=1+T=0$	$T=1+T=0$	$T=1$	$T=1$	$T=1$	$T=1$	
		s.p.e.	Expt.	$p<f$	Expt.	$p<f$	Expt.	$p<f$	
J_i	J_f	A	^{44}Ti	^{44}Ti	^{44}Ti	^{44}Ti	^{44}Ca	^{44}Ca	S.C.
2	0		116	179	74	138	12	16	(1)
4	2		1.4	1.4	1.1	1.5	0.7	0	1.4
6	4		1.2	1.4	0.5	1.5	0.3	0.5	1.6
8	6		0.9	1.2	0.6	1.4	0.6	0.8	1.6

placed in this deformed orbit. One cannot put two neutrons in the same orbit, but one can put a neutron and a proton in the same orbit. This means it is possible for a neutron-proton system to be more deformed than a proton-proton or neutron-neutron system. Thus, if there is a reasonably strong neutron-proton interaction, it is possible for the low-lying states to be deformed. The $T=0$ interaction acts only between a neutron and a proton, so it is not unreasonable to expect it to play an important role in determining whether or not a system displays collective rotational properties.

The calculations discussed in the previous section were made with the complete $T=0$ plus $T=1$ two-body residual interaction. In order to see what effect the $T=0$ interaction has on the calculations for ^{44}Ti, we have repeated the calculations with the $T=0$ matrix elements all set to 0. (This does not turn off the n-p interaction, since the $T=1$ force acts in the n-p system. If the $T=1$ interaction were turned off, there would be *no* n-n or p-p interactions.) With the $T=0$ interaction turned off, the structure of the low-lying states of ^{44}Ti were calculated with (a) the physical single-particle energies, and (b) with the p orbits degenerate and 2 MeV below the f orbits. The calculated spectra of the ground-state bands in these various models are shown in Fig. 4. In this figure, the energy of the 2^+ state in each spectra is normalized to 1 MeV. Compare first the ^{44}Ti calculation made with the full $T=0+T=1$ interaction and experimental s.p.e. with the calculation with only the $T=1$ interaction and experimental s.p.e. The two calculated spectra are qualitatively similar, the main difference being that the 6^+ and 8^+ states in the $T=1$ spectrum are relatively lower than in the spectrum with the complete interaction. However, although the spectra in these two models are similar, the wave functions are significantly different. In the complete $T=0+T=1$ interaction case, the $f_{7/2}{}^4$ $J=0$, $T=0$ component in the ground state constitutes about 48% of the wave function, and there are 16 components in the wave function, in the j-j basis we use, with amplitudes greater than 0.1. In the case of the calculation with only the $T=1$ interaction, the $f_{7/2}{}^4$ $J=0$, $T=0$ state constitutes 83% of the wave function, and there are six components in the wave function with amplitudes greater than 0.1. Thus, the $T=0$ interaction introduces a great deal of configuration mixing in the calculation, even though in this case the $T=0$ interaction does not make much apparent difference in the calculated excitation energies.

If we next consider the calculation for ^{44}Ti in which only the $T=1$ interaction is present, but the p orbits are lowered below the f orbits, we see that the spectrum appears to be much more rotational than is the case when the experimental s.p.e. are used with the $T=1$ interaction. In this case the wave function has 10 components with amplitudes greater than 0.1, and the two largest components are states in the $(p_{3/2}{}^4)$ and $(p_{3/2}{}^2, p_{1/2}{}^2)$ configurations. Each of these contribute about 25% to the total wave function. The $B(E2)$ values for these various models as calculated with the effective operator ($\epsilon_n=0.5$, $\epsilon_p=1.5$) described above are shown in Table III. We see that for both sets of single-particle energies, the strengths of the $B(E2)$'s are significantly reduced when the $T=0$ interaction is turned off. This is certainly a reflection of the importance of the $T=0$ interaction on the development of collective properties. However, it is worth noting that if we consider the calculation with only the $T=1$ interaction and experimental single-particle energies as an initial point, the change in the single-particle spectrum gives a larger increase in the $B(E2)$ value than does the addition of the $T=0$ interaction.

It is of interest to compare the structure of the low-lying states of ^{44}Ti obtained with only the $T=1$ part of the two-body interaction with that of the low-lying states of ^{44}Ca. This comparison partly brings out the effect of the Pauli principle on the deformation of the low-lying states of four nucleons outside ^{40}Ca. The two-body interaction will try to generate a deformed intrinsic state in both ^{44}Ca and ^{44}Ti. In ^{44}Ti, all four nucleons can occupy the lowest $K=\frac{1}{2}$ orbit, which has the largest quadrupole moment. In ^{44}Ca, however, the first two neutrons can occupy the $K=\frac{1}{2}$ orbit, but because of the Pauli principle, the other two neutrons must occupy the $K=\frac{3}{2}$ orbit, which has a smaller quadrupole deformation. Thus, although we use only the $T=1$ interaction in the calculation for both nuclei, we expect a larger deformation for ^{44}Ti. The spectra for this calculation are shown in the last four columns in Fig. 3. The ^{44}Ca spectrum is not rotational for either set of single-particle energies. For the case where the experimental single-particle energies are used, the spectra for ^{44}Ca and ^{44}Ti are quite similar. In the case when the p orbits are moved below the f orbits to form a situation favorable to the formation of states with large quadrupole deformation, the ^{44}Ti spectrum is distinctly more rotational than the ^{44}Ca spectrum. The $B(E2)$ values as calculated with the wave functions generated from the $T=1$ interaction are listed in Table III. The ^{44}Ti $B(E2)$ values are much larger than the analogous values for ^{44}Ca. One obvious reason is that ^{44}Ti has two protons with total charges three times the neutron charge, and this factor alone introduces large differences in the calculated $B(E2)$ values. In order to make more transparent the differences

in the calculated $B(E2)$ values in ^{44}Ti and ^{44}Ca which are due to the Pauli principle, we have repeated the $B(E2)$ calculations with the assumption that the neutron and proton have exactly equal charges. For the model space in which the $T=0$ interaction is turned off, and in which the single-particle spectrum is based on experimental evidence, the $B(E2)$ value in ^{44}Ti for the $2^+ \rightarrow 0^+$ transition is 1.6 times the $B(E2)$ value for the same transition in ^{44}Ca. In the model where the p orbits are 2 MeV below the f orbits, this ratio is 2.2. These results all point to a larger deformation of ^{44}Ti *vis-à-vis* ^{44}Ca in this model where only the $T=1$ parts of the residual interaction is operative, consistent with the arguments presented at the beginning of this paragraph.

VI. SUMMARY

In this paper we have presented the results of a conventional shell-model calculation of ^{44}Ti. The calculated spectrum is in reasonable agreement with available experimental data on the low-lying states of this nucleus. This theory-experiment comparison suggests the existence of a deformed rotational band starting at 1.90 MeV in ^{44}Ti. The results of the shell-model calculation have been compared with calculations of the structure of ^{44}Ti in terms of the stretch scheme and in terms of a PHF model. This comparison suggests that the PHF approach is not as effective here as in ^{20}Ne. Presumably this is because ^{44}Ti does not appear to be a "rotational" nucleus. There is no essential agreement between the shell-model calculation and the calculation in which the basis states are stretch-scheme states. The omission of important n-p correlations imposed by the stretch-scheme model used in that calculation is apparently critical.

Finally, we have discussed here some theoretical "experiments" which attempt to gain insight into the question of what factors are important in determining whether or not a given nucleus will display rotational properties. Most of the discussion is based on the assumption that if a nucleus displays rotational properties, the rotational states can be described as projections from an intrinsic deformed state. Certainly one important factor in these considerations is the fact that the quadrupole term is the dominant component in a multipole expansion of the residual interaction. This is true in all mass regions, but not all nuclei are rotational. Based on the projection from an intrinsic state idea, we have argued that the Pauli principle and the ordering of single-particle energies are important factors in dictating which nuclei are rotational. We have accumulated evidence that these arguments are valid by making a series of calculations with differing single-particle energies and with differing configurations of neutrons and protons. We have also studied the effect of the $T=0$ part of the residual two-body interaction by repeating these calculations with this $T=0$ interaction turned off. Taken together, these series of calculations imply that all these effects are significant in the formation of "rotational" properties. The strongest effects are due to the Pauli principle and the variation of the single-particle energies.

---

*Research sponsored by the U. S. Atomic Energy Commission under contract with Union Carbide Corporation.

†Present address: Physical Research Laboratory, Navrangpura, Ahmedabad-9, India.

[1]A. E. Litherland, J. Kuehner, H. Gove, M. Clark, and E. Almqvist, Phys. Letters 7, 98 (1961).

[2]M. Harvey, in *Advances in Nuclear Physics,* edited by M. Baranger and E. Vogt (Plenum Press, New York, 1969), Vol. 1.

[3]G. Ripka, in *Advances in Nuclear Physics,* edited by M. Baranger and E. Vogt (Plenum Press, New York, 1969), Vol. 1.

[4]E. C. Halbert, J. B. McGrory, B. H. Wildenthal, and S. P. Pandya, in Advances in Nuclear Physics (Plenum Press, New York, to be published), Vol. 4.

[5]S. B. Khadkikar and B. Banerjee, Nucl. Phys. A129, 220 (1969).

[6]M. Danos and V. Gillet, Phys. Rev. 161, 1034 (1967).

[7]J. B. French, E. C. Halbert, J. B. McGrory, and S. S. M. Wong, in *Advances in Nuclear Physics,* edited by M. Baranger and E. Vogt (Plenum Press, New York, 1969), Vol. 3.

[8]T. A. Belote, A. Sperduto, and W. E. Buechner, Phys. Rev. 139, 80 (1965).

[9]T. T. S. Kuo and G. E. Brown, Nucl. Phys. A114, 241 (1968).

[10]J. P. Elliot and T. H. R. Skyrme, Proc. Roy. Soc. (London) A232, 561 (1955).

[11]J. B. McGrory, B. H. Wildenthal, and E. C. Halbert, Phys. Rev. C 2, 186 (1970).

[12]J. Rapaport, J. B. Ball, R. L. Auble, T. A. Belote, and W. A. Dorenbusch, to be published; J. J. Simpson, W. R. Dixon, and R. S. Storey, Phys. Letters 30B, 478 (1969).

[13]M. A. Grace and A. R. Poletti, Nucl. Phys. 78, 273 (1966).

[14]J. Shah and M. Danos, Phys. Rev. 183, 899 (1969).

[15]S. A. Moszkowski, in *Handbuch der Physik,* edited by S. Flügge (Springer-Verlag, Berlin, Germany, 1967), Vol. 39, p. 411.